JOURNAL OF PROPULSION AND POWER
Vol. 17, No. 3, May–June 2001

Spectral Content of Solar Radiation on Martian Surface Based on Mars Pathfinder

J. Appelbaum* and A. Steiner†
Tel-Aviv University, 69978 Tel-Aviv, Israel
G. A. Landis‡ and C. R. Baraona§
NASA Glenn Research Center, Cleveland, Ohio 44135
and
T. Segalov†
Tel-Aviv University, 69978 Tel-Aviv, Israel

Photovoltaic arrays were used successfully to power the various instruments for the Mars Pathfinder. To identify the type of the solar cell most suitable for Mars surface missions in the future, the spectral content of Mars's solar radiation must first be determined. The response of photovoltaic cells depends on the solar cell type and the wavelengths of the incident light. The suspended dust particles of Mars's atmosphere affect the intensity and spectral content of the solar radiation reaching the planet's surface. The Pathfinder employed four bandpass filters for measuring the atmospheric optical depth during the course of the mission that lasted for about 80 sols (Martian days). The central wavelengths of these filters were 450, 670, 883, and 989 nm. This paper deals with the analysis of the optical depth of the Martian atmosphere based on the Mars Pathfinder measurements and includes 1) variation of the monochromatic optical depth with the time of the day, 2) variation of the monochromatic optical depth with sol for the duration of the mission, 3) variation of the optical depth with wavelength, 4) transmittance of the direct beam with wavelength, and 5) solar cell response on the Martian surface of the direct beam irradiance.

Nomenclature

a	=	semimajor axis of Mars orbit in astronomical units (i.e., $a = 1.5236915$)
b	=	ratio of atmospheric scale height to the planetary radius
c	=	coefficient
D	=	dust event duration
e	=	Mars eccentricity (i.e., $e = 0.093377$)
$I_{n\lambda}$	=	normal monochromatic direct-beam irradiance
$I_{\text{on}\lambda}$	=	extraterrestrial normal monochromatic spectral irradiance at the top of Mars's atmosphere
$I^E_{\text{on}\lambda}$	=	extraterrestrial spectral irradiance at mean sun–Earth distance
I_{sc}	=	short circuit current
J_{sc}	=	short circuit current density
L_s	=	areocentric longitude
$m(z)$	=	air mass
O_{da}	=	optical depth amplitude
P_{max}	=	power at maximum power point
r	=	sun–Mars distance
s	=	expectation of random variable
S_{dp}	=	sol of dust peak event
$\text{SR}(\lambda)$	=	spectral response of solar cell
$T(\lambda, \tau, z)$	=	monochromatic light transmittance
z	=	zenith angle
δ	=	declination angle
θ	=	true anomaly angle
λ	=	wavelength
$\tau(\lambda)$	=	monochromatic optical depth
σ	=	standard deviation
ϕ	=	latitude
ω	=	hour angle measured from the true noon westward; negative before noon and positive in the afternoon

Received 4 January 2000; revision received 30 June 2000; accepted for publication 11 July 2000.

*Professor, Faculty of Engineering.
†Student, Faculty of Engineering.
‡Research Scientist, Power Technology Division. Senior Member AIAA.
§Research Scientist, Power Technology Division.

I. Introduction

MISSIONS to Mars's surface will require electric power. Photovoltaic power systems offer many advantages, including high power-to-weight ratio, modularity, a long history of successful application in space, and so forth. The response characteristic of photovoltaic cells depends on the solar cell type and the spectral distribution of the incident light. Therefore, the amount of electricity produced by the solar cells, for a given amount of light energy, depends on the spectrum of the light source. Mars's atmosphere contains suspended dust particles that cause absorption and scattering of the solar radiation and thus affect the sunlight intensity and spectral content of the solar radiation reaching the surface of Mars.

The amount of dust in the Martian atmosphere varies with the presence of dust storms. Dust storms can be local (lasting only hours to days), regional, or global in extent, occurring for up to 100 days in duration. The global dust storms are seasonal and occur during the southern hemisphere summer (although not every summer will have such a dust storm). The best choice of solar cell for producing power during a global storm may be considerably different from the technology best suited for operation during clear periods. To identify the type of solar cell most suitable for Mars surface missions,[1] the spectral content of Mars solar radiation must first be determined.

The Mars Pathfinder spacecraft was launched in December 1996 and landed on the Mars surface on 4 July 1997, at Ares Villies, 19.5°N, 32.8°W, 850 km southeast of Viking Lander 1 (VL1 location 22.3°N, 47.9°E). The Pathfinder was equipped with various instruments, including an instrument to measure the optical depth of Mars atmosphere. This Imager for Mars Pathfinder (IMP) employed four narrow, widely separated bandpass solar filters for measuring the atmospheric optical depth during the course of the mission. Smith et al.[2] have described the IMP. The center wavelengths of the four filters are 450.3, 669.8, 883.4, and 988.9 nm with bandwidths of 4.91, 5.30, 5.60, and 5.39 nm (see solar filter relative spectral response in Ref. 2), respectively.

The IMP is a principal investigative instrument for the Mars Pathfinder spacecraft. The IMP is a stereo imaging system with color capability provided by a set of selective filters for each of the two camera channels. It consists of three physical subassemblies: 1) camera head (with stereo optics, filter wheel, CCD and preamp, mechanism and stepper motors), 2) extendable mast with electronic cabling, and 3) two plug-in electronics cards (CCD data card and power-supply motor-drive card). Azimuth and elevation drives for the camera head are provided by stepper motors with gear heads, providing a field of observation of $\pm 180°$ in azimuth and $+83°$ to $-72°$ in elevation, relative to lander coordinates. The azimuth and elevation capabilities of the camera are related to viewing of the sky information and hence on the extent of the spectral content of the atmosphere information. The camera system is mounted at the top of a deployable mast, and when it is deployed, the elevation is 1.75 m above the ground. The IMP has been characterized and calibrated with respect to absolute responsivity, spectral response, image quality, flat fielding, dark current, stray light, geometric image characteristics and alignment, and absolute pointing. Measurements of the optical depth[3] were made by these filters several times on most sols (Martian days), typically on the hour from 0700 to 1700 hrs Local Solar Time (LST). After sol 30, the lander was turned off after downlink (typically 1400 to 1500 hrs), and therefore there are limited data after 1400 hrs and almost no data before 0900 hrs. The measurements were recorded during the mission that lasted for about 80 sols, corresponding to L_s 143° to L_s 187° (late summer in the northern hemisphere). The measured solar intensities were used to derive the optical depth by applying Beer's Law.[3] It includes, among others, corrections for the varying distance to the sun and temperature variation affecting the center wavelength and bandwidth of the solar filters. The error reported in the optical depth is typically 2%. The spectral content of Mars's solar radiation analyzed in this paper is based on these optical depths.[3]

The optical depths for the four wavelengths were determined from images of the sun; therefore, the spectral content of the Martian atmosphere corresponds to the direct-beam irradiance. The spectral content of the indirect (diffuse) component of the sunlight is spectrally shifted toward the red and varies with the angular separation from the sun.[4] It should be emphasized that at low optical depths of about 0.5, the diffuse irradiance contributes about 34% to the global irradiance at the surface. Therefore, the spectral content of the direct-beam irradiance has a greater effect on the solar cell response at low optical depths.

We have analyzed the optical depth of 53 sols, among them 37 with data in the morning and in the afternoon, 11 sols with data only in the morning, and 5 sols with data only in the afternoon. For the other sols, the data were either not recorded or given for a limited number of points.

In this article we analyze 1) variation of the optical depth (for the four wavelengths) with the time of the day, 2) variation of the optical depth with sol for the duration of the mission, 3) variation of the optical depth with wavelength, 4) transmittance of the direct beam with wavelength, and 5) solar cell response on the Martian surface of the direct-beam irradiance.

II. Extraterrestrial Spectral Irradiance on Mars

The spectral distribution of the extraterrestrial radiation is the radiation that would be received at the sun–Mars mean distance in the absence of the atmosphere. In other words, it is the spectral energy per unit of time received on a unit area of surface perpendicular to the direction of propagation of the radiation at the mean sun–Mars distance, outside the atmosphere. The irradiance, in W/m^2 is given by

$$I_{\mathrm{on}\lambda} = I^E_{\mathrm{on}\lambda} \Big/ r^2 \tag{1}$$

where $I_{\mathrm{on}\lambda}$ is the extraterrestrial (o), normal (n), monochromatic (λ) spectral irradiance at the top of Mars's atmosphere; $I^E_{\mathrm{on}\lambda}$ is the extraterrestrial spectral irradiance at mean sun–Earth distance; and r is the instantaneous sun–Mars distance, in astronomical units (AU), given by

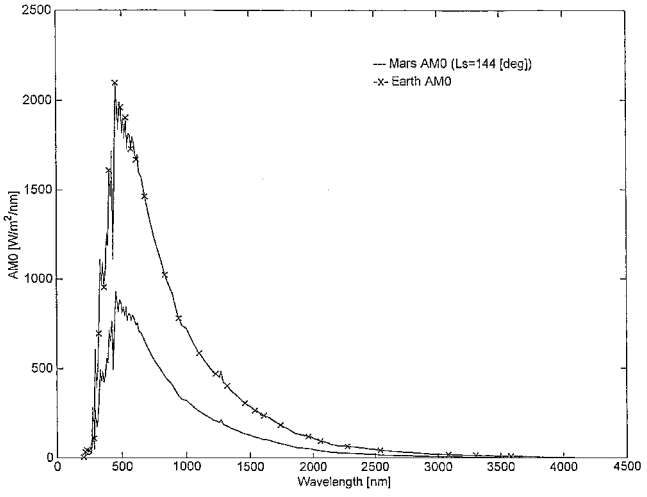

Fig. 1 Extraterrestrial spectral irradiance on Earth (AM0) and on Mars (AM0) for L_s = 144°.

$$r = \frac{a(1-e^2)}{1+e\cos\theta} \tag{2}$$

The angle θ is given by

$$\theta = L_s - 248° \tag{3}$$

where L_s is the areocentric longitude and 248° the areocentric longitude of Mars perihelion.

The extraterrestrial spectral irradiance on Earth (AM0) is shown in Fig. 1. The extraterrestrial irradiance on Mars (AM0) for $L_s = 144°$, calculated by using Eqs. (1) and (2), is also shown in this figure. The areocentric longitude $L_s = 144°$ corresponds to sol 3 on 7 July 1997, that is, three Martian days (sols) after the Pathfinder landing on the surface of Mars.

III. Spectral Irradiance on the Martian Surface

According to Beer's law, the intensity of a monochromatic beam of light through a medium of constant optical properties decreases exponentially with the distance traversed in the medium. The distance traversed in the medium is called the air mass, $m(z)$. Beer's law applies in most instances, whether the energy is absorbed or scattered. In terms of this law,

$$I_{n\lambda} = I_{\mathrm{on}\lambda} \exp[-\tau(\lambda)m(z)] \tag{4}$$

where $I_{\mathrm{on}\lambda}$ is the normal, monochromatic, direct-beam irradiance at the top of Mars's atmosphere; $I_{n\lambda}$ is the normal, monochromatic, direct-beam irradiance on the Martian surface; and $\tau(\lambda)$ is the monochromatic optical depth.

For most cases of interest, the air mass is defined as

$$m(z) = 1/\cos z \tag{5}$$

This approximation is excellent for z from 0° to 80°. For zenith angles close to 90° (sunrise or sunset) a more accurate expression is

$$m(z) = [(b^2\cos^2 z + 2b + 1)^{\frac{1}{2}} - b\cos z] \tag{6}$$

where b is the ratio of atmospheric scale height to the planetary radius ($b \cong 314$ for Mars).

The zenith angle is the angle between the vertical and the line to the sun given by

$$\cos z = \sin\phi\sin\delta + \cos\phi\cos\delta\cos\omega \tag{7}$$

where

$$\omega = 15 \cdot \mathrm{LST} - 180° \tag{8}$$

where LST is Mars local solar time and the solar declination angle is given by

$$\sin\delta = \sin 24.936^\circ \sin L_s \tag{9}$$

The monochromatic transmittance coefficient $T(\lambda)$ is the ratio of radiation emerging from a medium to incident radiation. The monochromatic transmittance due to direct-beam irradiance on a surface normal to the sun's rays may be written as

$$T(\lambda) = I_{n\lambda}/I_{\mathrm{on}\lambda} \tag{10}$$

From Eqs. (4) and (10), we obtain

$$T(\lambda, \tau, z) = \exp[-\tau(\lambda)m(z)] \tag{11}$$

indicating that the transmittance is a function of wavelength, optical depth, and zenith angle.

IV. Characteristic Optical Depth

The data of the optical depth of the four wavelengths contain dust devils or turbulences (transient events) lasting for short periods. From the observation of the optical depth throughout the mission, one may notice a characteristic variation of the optical depth with time of day and with the sol during the mission. Figure 2 shows the variation of the measured optical depths for the four wavelengths at 1000 hrs LST. An oscillatory behavior may be noticed during the mission by looking, for instance, at the 450 nm wavelength marked by the solid circles. We are interested in the general behavior of the optical depth, therefore we define a characteristic optical depth (COD). We assume that changes in the optical depth during the day, and from day to day, occurred gradually. The motivation for obtaining a COD was to learn about the trend in the optical depth variation for each wavelength during the different days as the mission progressed. The COD may be mathematically represented containing the sol (or L_s), LST, and λ. The form of the mathematical expression (model) resembles that used by Appelbaum et al.[5] for the optical depths

$$\begin{aligned}\mathrm{COD(LST, sol)} = {} & \left[O_{\mathrm{da1}} \cdot \exp\left\{-(\mathrm{sol} - S_{\mathrm{dp1}})^2 \big/ D_1\right\}\right. \\ & + O_{\mathrm{da2}} \cdot \exp\left\{-(\mathrm{sol} - S_{\mathrm{dp2}})^2 \big/ D_2\right\} \\ & + O_{\mathrm{da3}} \cdot \exp\left\{-(\mathrm{sol} - S_{\mathrm{dp3}})^2 \big/ D_3\right\} \\ & \left. + O_{\mathrm{da4}} \cdot \exp\left\{-(\mathrm{sol} - S_{\mathrm{dp4}})^2 \big/ D_4\right\}\right] \\ & \times \left[O_{\mathrm{da5}} \cdot \exp\left\{-(\mathrm{LST} - S_{\mathrm{dp5}})^2 \big/ D_5\right\} + \exp\left\{-(\mathrm{LST}\right.\right. \\ & \left.\left. - S_{\mathrm{dp6}})^2 \big/ D_6\right\}\right] \cdot \cos(\pi \cdot \mathrm{LST}/24 \cdot D_7 + 0.5\pi) + \mathrm{base}\end{aligned} \tag{12}$$

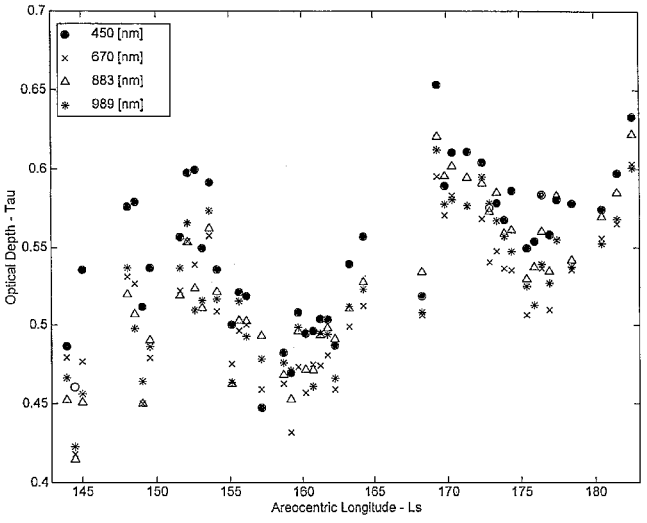

Fig. 2 Measured optical depth for the four wavelengths at 1000 hrs LST.

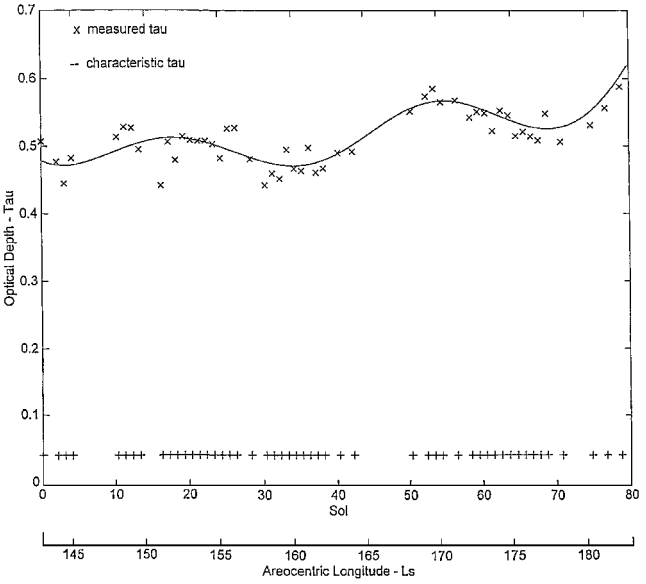

Fig. 3 Measured and characteristic optical depth for 670 nm at 1200 hrs LST along the Pathfinder mission.

where O_{da}, S_{dp}, and D are coefficients for a given wavelength; LST is the local solar time; and sol is the day number. O_{da} are coefficients of optical depth amplitude, S_{dp} are coefficients of sol of dust peak event, and D are coefficients of dust event duration; base is an optical depth offset parameter, and the cosine term corresponds to symmetry around noon.

The COD model is based on the statistical behavior of the measured optical depth during the mission. One may observe that all dust events have a Gaussian distribution around the dust event peaks (see Appendix A; Ref. 6). An important parameter of the COD is the "base" value, which is a minimal value of optical depth during the mission. Therefore, the COD model may be described as a Gaussian process above a minimum level of no dust activity. Equation (12) is a three-dimensional function of COD, LST, and sol number, with 19 fitting coefficients for each of the 4 wavelengths. The coefficient values were obtained by fitting Eq. (12) to all the measured optical depth for the above-mentioned 53 sols using the minimum mean square error (MMSE) algorithm.[7] A table of the coefficients is given in Appendix B. Figure 3 shows the measured and the characteristic optical depths, for example, for the 670 nm wavelength between 1130 hrs and 1230 hrs LST and clearly indicates the general variation of the COD formulated by Eq. (12) with respect to the measurement. Other wavelengths behave similarly. Figure 3 also includes an indicator (horizontal + + + line) showing days for which the optical depth was measured and included in the analysis, and blanks where either no measurements of the optical depth were performed by the IMP or sols with very few measurements were not considered in the derivation of the COD. The mathematical representation of the COD predicts missing data. It should be remembered that the instantaneous value of the optical depth is given by the measurements and the general variation is given by the COD.

V. Diurnal Variation of the Optical Depth

The measured and the characteristic optical depths for the four wavelengths are shown in Figs. 4 and 5, respectively, for sol 15 (early in the mission) and in Figs. 6 and 7, respectively, for sol 68 (late in the mission). The standard deviation error of the measured optical depth with respect to the COD is 5% on the average. The standard deviation for sol 15 is 2.29% for 450 nm, 3.51% for 670 nm, 3.50% for 883 nm, and 4.40% for 989 nm (see Appendix B). For sol 68, it is 3.27% for 450 nm, 2.16% for 670 nm, 1.94% for 883 nm, and 1.97% for 989 nm. A cloud or a dust devil event is observed on sol 13, Fig. 8, at about 1100 hrs. This dust event does not appear in the COD as seen in Fig. 9 because the COD represents the general behavior of the optical depth and therefore filters out, by its nature, any transients. As mentioned, the COD may also predict

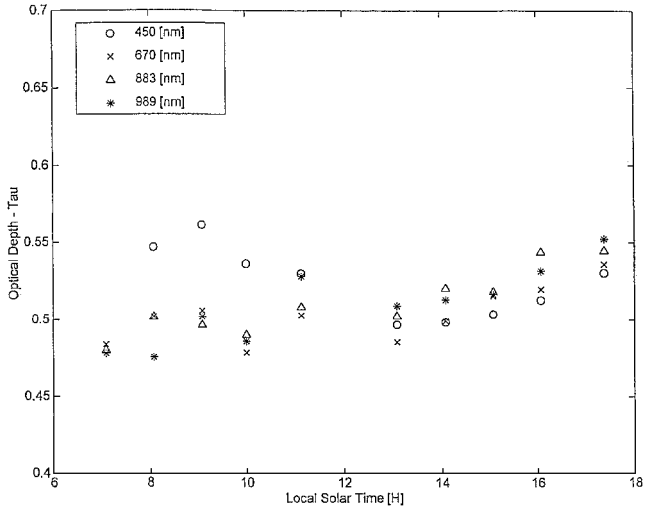

Fig. 4 Measured spectral optical depth for four wavelengths (450, 670, 883, and 989 nm) for sol 15.

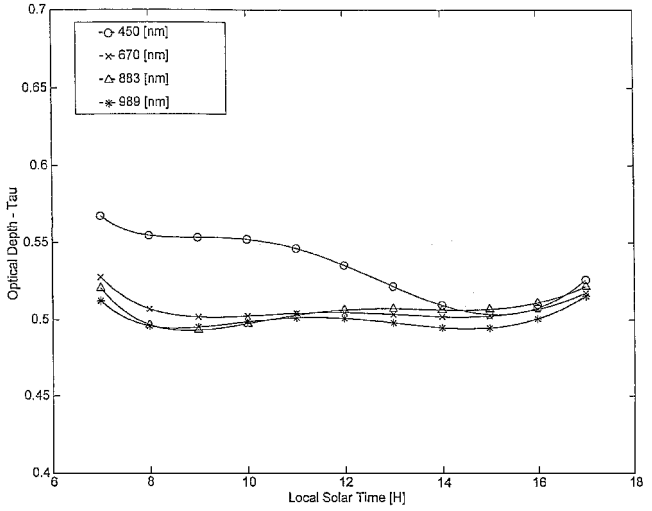

Fig. 5 Characteristic spectral optical depth for four wavelengths (450, 670, 883, and 989 nm) for sol 15.

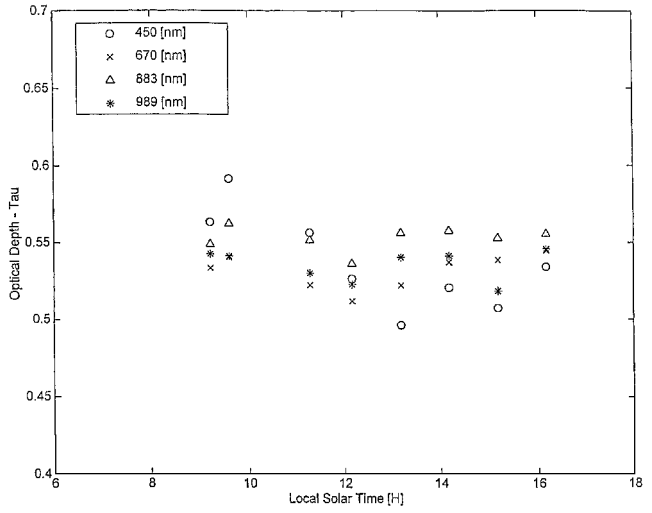

Fig. 6 Measured spectral optical depth for four wavelengths (450, 670, 883, and 989 nm) for sol 68.

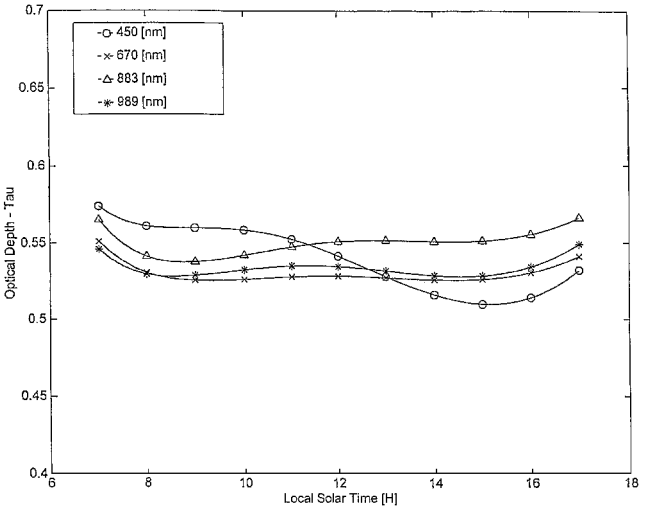

Fig. 7 Characteristic spectral optical depth for four wavelengths (450, 670, 883, and 989 nm) for sol 68.

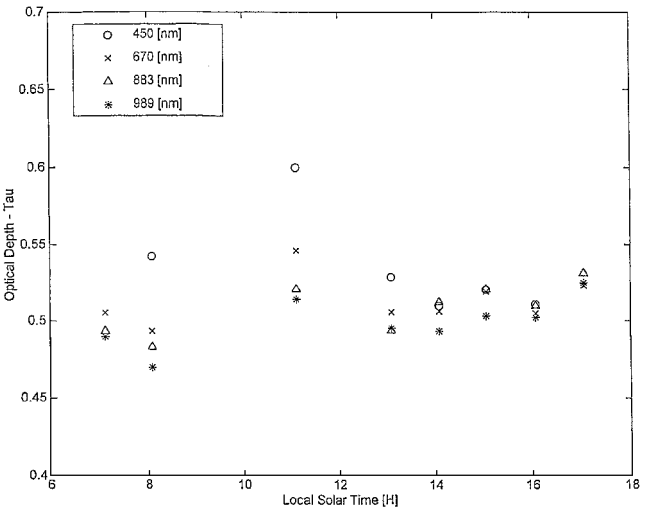

Fig. 8 Measured spectral optical depth for four wavelengths (450, 670, 883, and 989 nm) for sol 13.

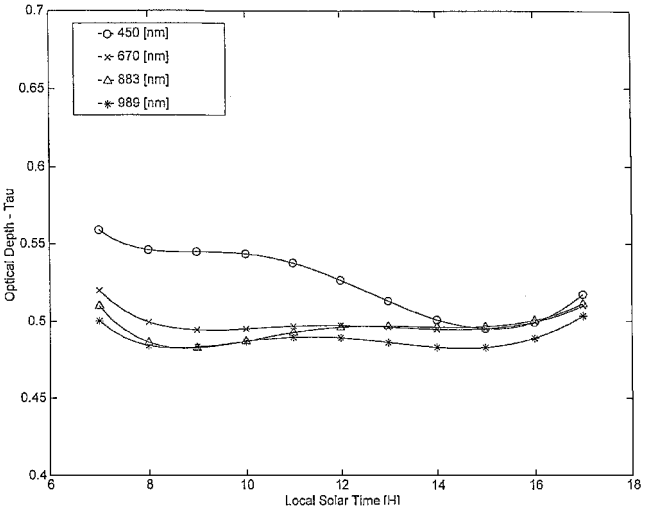

Fig. 9 Characteristic spectral optical depth for four wavelengths (450, 670, 883, and 989 nm) for sol 13.

missing (or not measured) measurements, as seen in Figs. 8 and 9 for sol 13.

We have analyzed the optical depth of 53 sols and calculated their COD. Larger variation in optical depth for the 450 nm wavelength is seen before noon than in the afternoon (see Figs. 5 and 9) at the beginning of the mission, up to about sol 22. For the other wavelengths, the variation is rather small. The optical depth of the 450 nm wavelength is significantly higher in the morning than for the other wavelengths up to about sol 15; the lowest optical depth is for the wavelength 989 nm (Figs. 5 and 9). For sols later than sol 15, the optical depth for 450 nm is the highest in the morning and becomes the lowest in the afternoon; the optical depth for 883 nm is the second highest in the morning and becomes the highest in the afternoon (see Fig. 7). After sol 23, the optical depths vary similarly for all wavelengths (see Fig. 7).

These results were obtained from the analysis of COD and agrees, at large, with the optical depths measured by the IMP and analyzed by Smith and Lemmon.[3] The higher optical depth in the morning comes primarily in blue light (450 nm) and is indicative of small particles scattering. These particles are probably water-ice condensation that sublimates in time throughout the early afternoon.

VI. Daily Variation of the Optical Depth

The variation of the COD with the sol number for 80 days for the four wavelengths is shown in Figs. 10, 11, and 12, for 0800, 1200, and 1600 hrs LST, respectively. The COD shows the variation of the optical depth for each wavelength throughout the mission and for which wavelength the optical depth is higher in the morning and lower in the afternoon; it may also predict the optical depth shortly before and after the mission. The same general behavior holds for other hours. We may conclude from these figures that the optical depth cycled and increased during the mission from about 0.45 to about 0.65. One may interpret that during the 80 sols two storm events occurred, one peaking on about sol 20 and the other peaking on about sol 55 and lasting for about 25 to 30 sols. The dust events began around sols 10 and 40 and ended around sols 35 and 70. A lower value of optical depth probably took place before landing, and a higher peak probably occurred after the IMP ceased to function. The intensity of the storm events increased with the mission, as seen by the increasing slopes of the optical depth from about 4.5×10^{-3}/sol to 7.25×10^{-3}/sol to 15.5×10^{-3}/sol.

Figure 9 shows that the highest optical depth is for 450 nm for all sols. At midday (Fig. 10) the 883 nm becomes the highest optical depth and the 670 nm becomes the lowest. At 1600 hrs (Fig. 11), the highest optical depth is for 883 nm and the lowest is for 450 nm. This

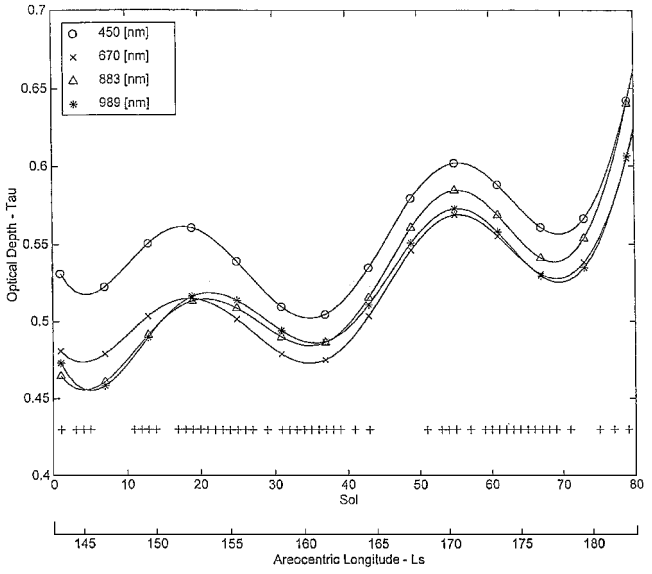

Fig. 10 Variation of the characteristic spectral optical depth with the sol number along the Pathfinder mission for four wavelengths (450, 670, 883, and 989 nm) at 0800 hrs LST.

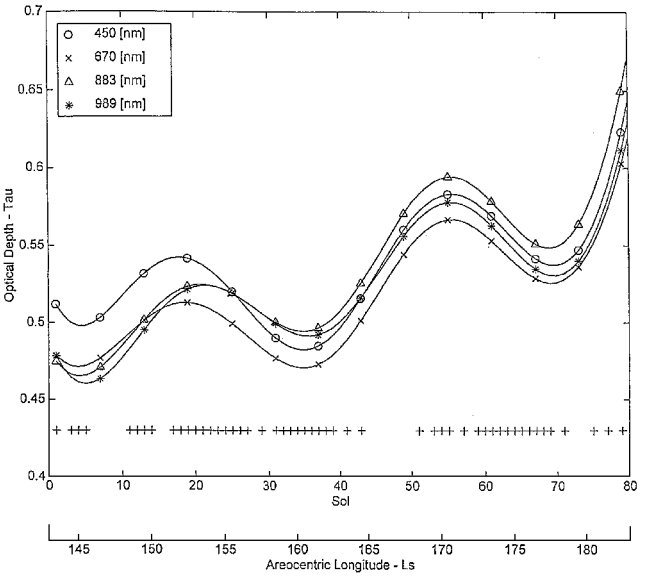

Fig. 11 Variation of the characteristic spectral optical depth with the sol number along the Pathfinder mission for four wavelengths (450, 670, 883, and 989 nm) at 1200 hrs LST.

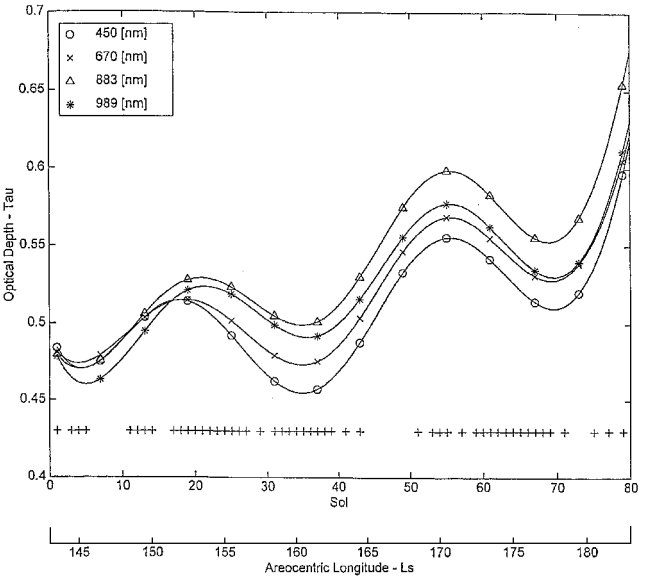

Fig. 12 Variation of the characteristic spectral optical depth with the sol number along the Pathfinder mission for four wavelengths (450, 670, 883, and 989 nm) at 1600 hrs LST.

happens at about 1300 hrs and lasts until the end of the day. The sublimation of ice particles during the midmorning hours (decrease in 450 nm optical depth) projects the effect of spectral shift toward the red (883 nm) caused by the suspended dust in the afternoon hours.

The fitting of the COD to the measured values for the entire mission is very good. The standard deviation average error is 6.11% for 450 nm, 5.24% for 670 nm, 5.63% for 883 nm, and 5.31% for 989 nm (see Appendix B). It should be emphasized that the fitting process takes into account a great deal of the relevant measured optical depths for the entire mission, resulting in a standard deviation average. A single measured point may deviate, of course, from this average.

VII. Variation of Optical Depth with Wavelength

The dependence of the COD on wavelength is of interest. This dependence is also needed to determine the transmittance of the atmosphere to solar irradiance (Eq. 11). Within the wavelength range of the IMP, the atmospheric scattering is due only to aerosols.[8] Rayleigh scattering by the gas molecules can be neglected without

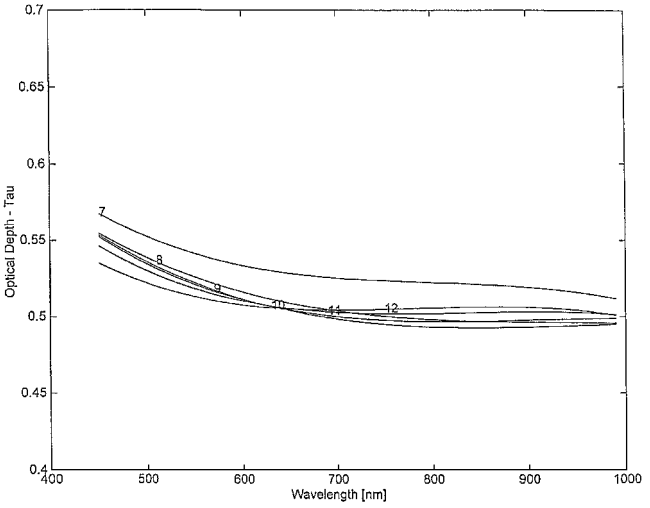

Fig. 13 Variation of the COD with wavelength for forenoon hours for sol 15.

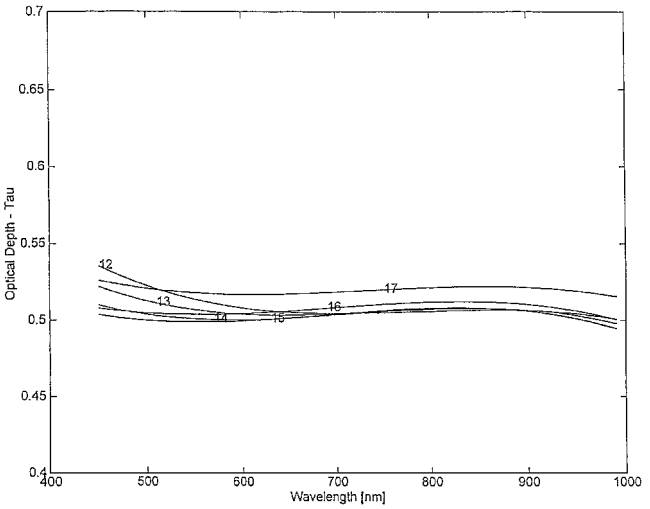

Fig. 14 Variation of the COD with wavelength for afternoon hours for sol 15.

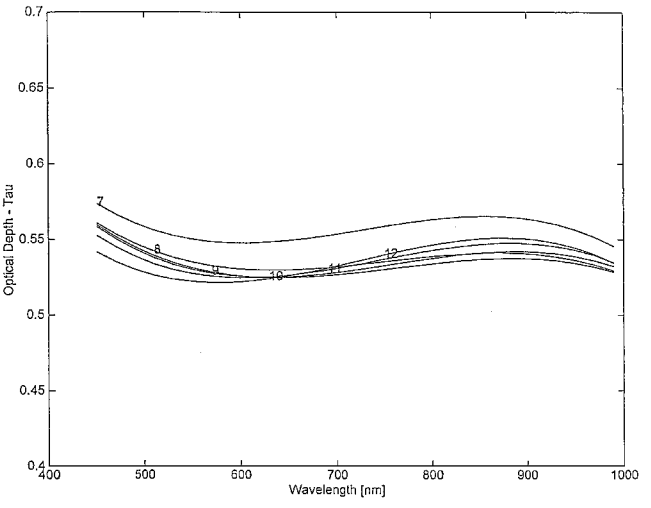

Fig. 15 Variation of the COD with wavelength for forenoon hours for sol 68.

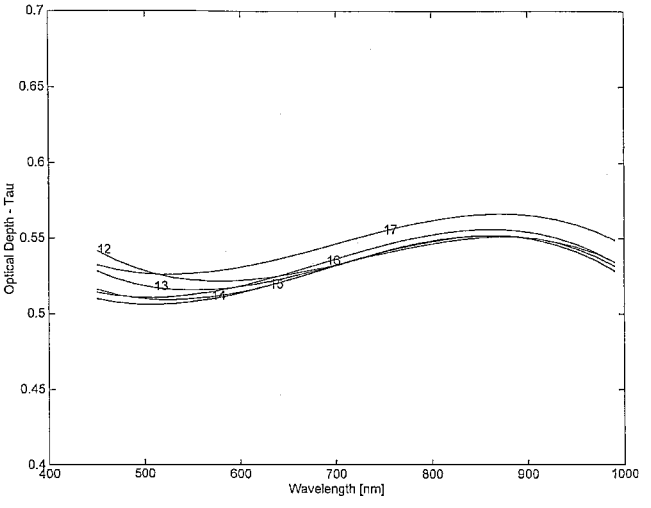

Fig. 16 Variation of the COD with wavelength for afternoon hours for sol 68.

introducing any noticeable error. Judging from the data, the aerosols can be expected to be primarily dust particles. The variation of the COD with wavelength was obtained by spline interpolation between the measured optical depths for the four wavelengths. It was assumed that the variation is monotonic. This may be explained by the attenuation of the solar irradiance, which is mainly due to a single constituent (dust) of the Martian atmosphere.

Figures 13 and 14 show the COD for sol 15 before noon and for the afternoon, respectively; the parameter is the hour of the day (LST). For the morning hours (0700 to 1200), the COD is higher for shorter wavelengths. In the afternoon (1200 to 1700 hrs), the dependence of the COD on wavelength is minor. This behavior is observed up to about sol 25. One may notice that at about 900 nm the COD starts to decrease. This is more pronounced in higher sols. Figures 15 and 16 show the variation of the characteristic optical depth for sol 68. Before noon, the COD changes slightly for all wavelengths and obtains a lower value at about 650 nm and a higher value at about 900 nm. In the afternoon, the COD increases with the wavelength, having a maximum at about 900 nm.

VIII. Transmittance Variation of Direct-Beam Irradiance with Wavelength

The transmittance of the solar irradiance as a function of wavelength is of interest. This dependence is also needed for the calculation of the short circuit current of solar cells.

The transmittance $T(\lambda, \tau, z)$ of the direct-beam irradiance (Eq. 11) was calculated based on the COD obtained in Sec. VII. Up to about sol 21, the transmittance increases gradually with wavelength for the morning hours as shown in Fig. 17 for sol 15. In the afternoon (Fig. 18), the transmittance is almost constant. For sols later than sol 21, the transmittance is almost constant for the morning hours but decreases in the afternoon for wavelengths up to about 900 nm, as shown in Figs. 19 and 20 (sol 68), respectively. One may notice a slight decrease in transmittance with a minimum at about 900 nm. The variation of transmittance with the time of the day follows the variation of the direct-beam solar irradiance on the surface of Mars [Eqs. (1), (4), and (11)].

IX. Relative Performance of Gallium Arsenide and Silicon Solar Cells on the Martian Surface

The short circuit current density of a solar cell is defined by

$$J_{sc} = \int_{\lambda_1}^{\lambda_2} I_{on\lambda}(\lambda) T(\lambda) \mathrm{SR}(\lambda)\, \mathrm{d}\lambda \tag{13}$$

where $\mathrm{SR}(\lambda)$ is the spectral response of the solar cell and $I_{on\lambda}(\lambda)$ and $T(\lambda)$ are given by Eqs. (1) and (11), respectively. Measurements of silicon (Si) and gallium arsenide (GaAs) solar cells were performed at NASA Glenn Research Center. These measurements include variation of the short circuit current, open circuit voltage,

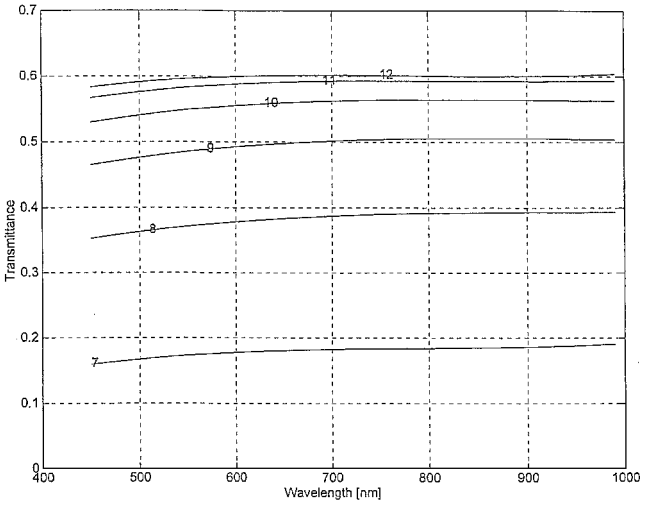

Fig. 17 Variation of the direct-beam transmittance with wavelength for forenoon hours for sol 15.

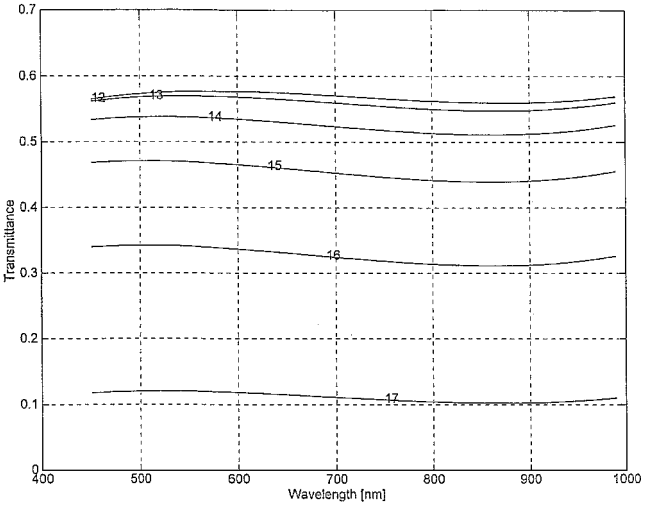

Fig. 20 Variation of the direct-beam transmittance with wavelength for afternoon hours for sol 68.

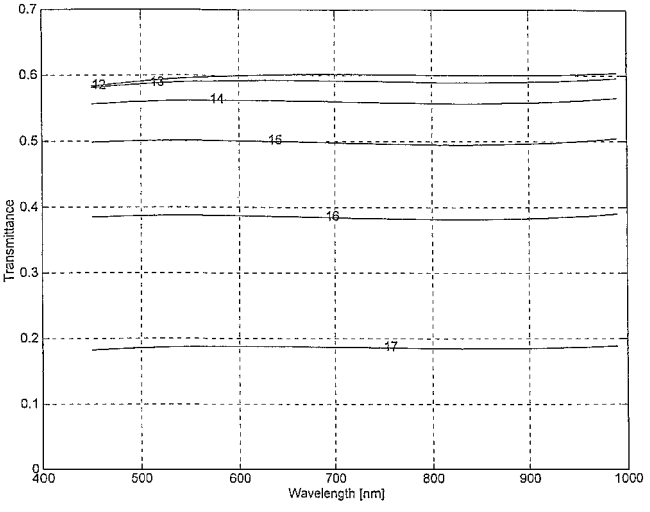

Fig. 18 Variation of the direct-beam transmittance with wavelength for afternoon hours for sol 15.

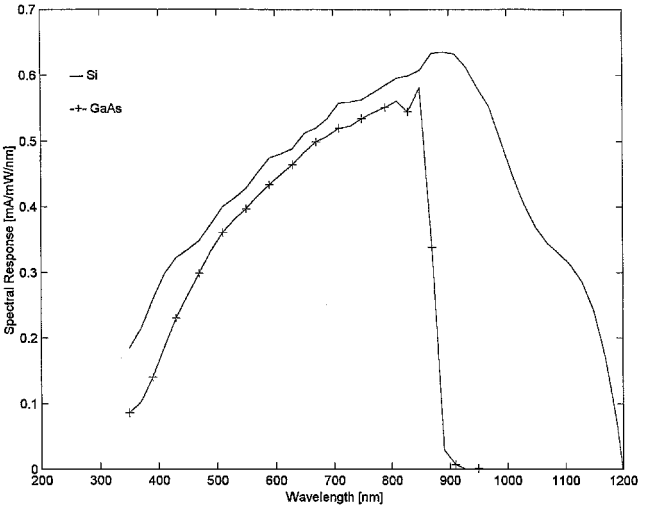

Fig. 21 Spectral response of Si and GaAs solar cells.

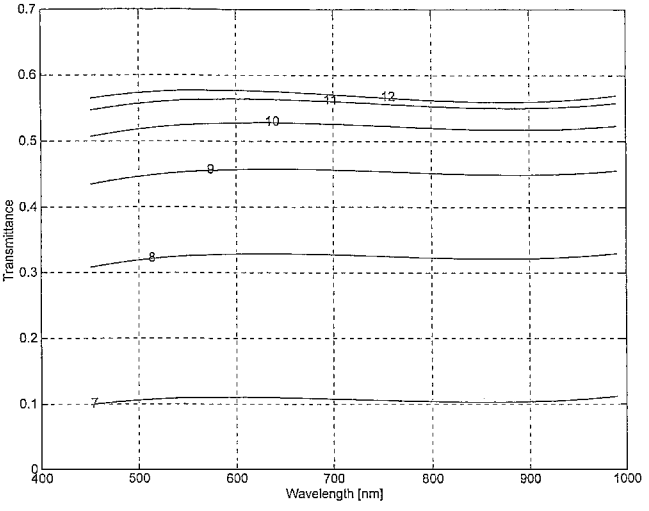

Fig. 19 Variation of the direct-beam transmittance with wavelength for forenoon hours for sol 68.

and the maximum power with irradiance, as well as the spectral response. All measurements were done at 25°C. One Si cell and one GaAs cell of close efficiencies were chosen for the comparison in the present study. The efficiencies of Si and GaAs cells at AM0 are 19% and 18.43%, respectively, and the spectral responses are shown in Fig. 21.

The measurements of the solar cells show a linear dependence (with a good approximation) of the short circuit current and the maximum power with irradiance. Consequently, the maximum power is also linearly dependent on the short circuit current, i.e., $P_{\max} = cI_{\mathrm{sc}}$. We compare the short circuit current and maximum power of these solar cells, taking into account only the spectral content of the direct-beam solar irradiance and not considering other factors affecting the solar cell efficiency. It should be noted that the indirect component of the light (diffuse irradiance) may also introduce a spectral shift to the spectral content of the solar irradiance reaching the surface of Mars. Figure 22 shows the diurnal variation of the short circuit current density for the Si and GaAs solar cells for sols 15 and 68, indicating that the short circuit current for the Si cell is higher than that for the GaAs cell. This figure was obtained from Eq. (13) and Figs. 17 to 21.

From the laboratory measurements of the above-mentioned two solar cells, we obtained the relationship between the power at maximum power point and the short circuit current density:

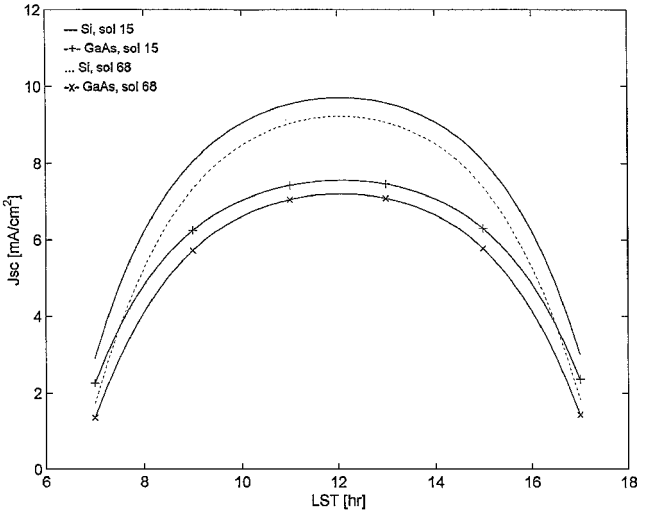

Fig. 22 Diurnal variation of the short circuit current density of Si and GaAs solar cells for sols 15 and 68.

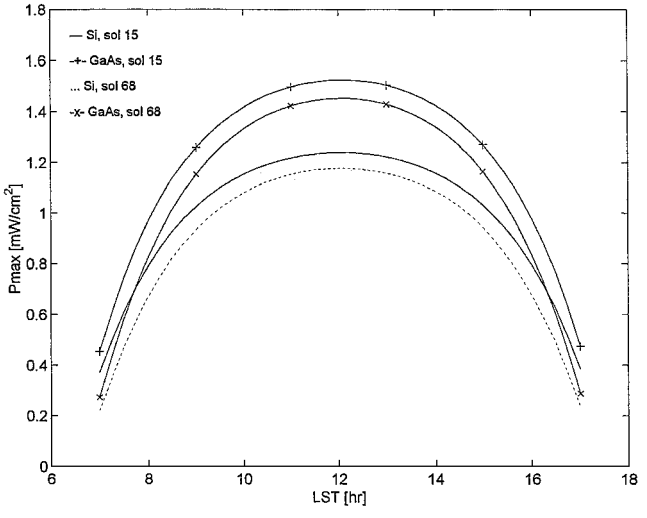

Fig. 23 Diurnal variation of the power at the maximum power point of Si and GaAs solar cells for sols 15 and 68.

$$P_{\max}^{\mathrm{Si}}(\mathrm{mW/cm^2}) = 0.12753 J_{\mathrm{sc}} \qquad (\mathrm{mA/cm^2})$$

$$P_{\max}^{\mathrm{GaAs}}(\mathrm{mW/cm^2}) = 0.20137 J_{\mathrm{sc}} \qquad (\mathrm{mA/cm^2}) \qquad (14)$$

The diurnal variation of $P_{\max}$ for the Si and GaAs solar cells for sols 15 and 68 is shown in Fig. 23, indicating the advantage of the GaAs solar cell.

X. Conclusions

During its operation on the Martian surface, the IMP returned sequences of images of the Martian sky capable of characterizing the size distribution, optical constants, and nature of the aerosols suspended in the planet's atmosphere. The optical depths of the Martian atmosphere at the four wavelengths (450, 670, 883, and 989 nm) were determined from images of the sun. The measurements were made several times on most sols. In comparison, the optical depth of the Viking Lander was measured only twice a sol and at one wavelength (670 nm). However, the Viking Lander operated for more than a year and experienced large variation in dust activities, whereas the Mars Pathfinder operated about 80 days during a period of a relatively calm atmosphere. The optical depth cycled and increased during the mission from about 0.45 to about 0.65. A solar radiation model was developed based on the Viking Lander measurements. With the new data from the Mars Pathfinder, one may improve the solar radiation model, at least for the period when the mission took place.

To analyze the spectral content of the solar radiation on the Martian surface, we introduced a COD of Mars's atmosphere for the mission, expressed analytically and representing a general behavior of the optical depth with time of day and with sol for each wavelength. The COD may differ locally from the measured optical depth at a particular point; however, the COD gives the general behavior of the optical depth during the mission, from which conclusions may be drawn because this mathematical expression (COD) was derived from all measured relevant points during the mission. The Mars Pathfinder mission took place at a period of low dust activity on Mars; therefore, the optical depth for each wavelength varied in a narrow range.

The variation of the optical depth with time of day, with sol, and with wavelength is of interest and was one of the aims of the Mars Pathfinder mission. The variation of the optical depth with wavelength is used also in this study to compare the relative performance of Si and GaAs solar cells. It should be noted that this comparison is limited for two reasons: The spectral variation of the Martian atmosphere is small in the range of the variation of the optical depth (0.45 to 0.65), and the spectral variation corresponds only to the direct-beam irradiance. Because Mars's atmosphere contains mainly suspended dust particles, the diffuse component of the irradiance becomes more significant for higher optical depths, and with it, the spectral variation increases. For low optical depth (clear skies) encountered during the Mars Pathfinder mission, the variation of the spectral content of the solar radiation was small; therefore, one cannot conclude which is the preferred solar cell for Mars surface operation.

Appendix A: Gaussian Probability Distribution of Characteristic Dust Events

Observation of a dust storm event during a period (several days before and after a dust peak) resembles a Gaussian probability distribution function.[6]

$$f(x) = \left(1/\sqrt{2\pi\sigma^2}\right)\exp[-(x-s)^2/2\sigma^2] \qquad (A.1)$$

where x is the Gaussian random variable; s is the expectation of x; σ^2 is the expectation of x^2, variance; and σ is the standard deviation of x.

In terms of the dust event parameters (O_{da}, S_{dp}, and D), we define a characteristic dust event (CDE) according to Eq. (A.1) by

$$\mathrm{CDE} \triangleq O_{\mathrm{da}} \exp\left[-(\mathrm{sol} - S_{\mathrm{dp}})^2 / D^2\right] \qquad (A.2)$$

and

$$D = \sqrt{2}\sigma \qquad (A.3)$$

where D is a dust event duration and represents an approximation of the duration of a dust event, and σ is the standard deviation of the dust event. The COD differs from a Gaussian distribution function mainly in the cumulative function:

$$\int_{-\infty}^{\infty} f(x)\,\mathrm{d}x = 1 \qquad (A.4)$$

We obtain

$$O_{\mathrm{da}} \cdot \int_{-\infty}^{\infty} \exp\left[-(\mathrm{sol} - S_{\mathrm{dp}})^2 / D^2\right] d(\mathrm{sol}) = \sqrt{\pi} D O_{\mathrm{da}}$$

Thus, $\sqrt{(\pi)} D O_{\mathrm{da}}$ is the significance of the dust storm event and represents its intensity.

The standard deviation error of the COD with respect to the measured optical depth (OD) is given by

$$\sigma = \left[\frac{1}{M}\sum(\mathrm{OD}_i - \mathrm{COD}_i)^2\right]^{\frac{1}{2}} \qquad (B.1)$$

Appendix B: Coefficients of Characteristic Optical Depth Equation

Table 1 Coefficients of COD, Eq. (12)

Wavelength, nm	O_{da1}	O_{da2}	O_{da3}	O_{da4}	O_{da5}	S_{dp1}	S_{dp2}	S_{dp3}	S_{dp4}	S_{dp5}	S_{dp6}
450	71.129	198.209	−26.163	700.000	0.042	−8.079	54.555	54.839	383.000	203.000	−16.134
670	74.532	193.673	−22.903	700.000	0.047	−8.372	54.134	54.672	383.000	6.339	−16.792
883	104.735	245.295	−25.648	700.000	0.028	−9.473	55.597	55.097	383.000	7.037	−21.150
989	75.452	192.455	−21.696	700.000	0.044	−7.000	55.504	55.256	383.000	6.407	−16.714
Wavelength, nm	D_1	D_2	D_3	D_5	D_5	D_6	D_7	Base	Standard deviation, %		
450	578.494	5170.958	413.269	400.000	470.168	159.061	3.325	4.220	6.11		
670	624.290	5168.316	312.636	400.000	468.784	182.836	5.846	3.053	5.24		
883	763.086	5135.727	311.058	400.000	546.548	223.608	3.433	3.913	5.63		
989	629.146	5169.315	330.033	400.000	464.682	175.037	4.285	3.632	5.31		

where the ith measured and COD correspond to a given sol and time (LST) and M is the total number of relevant measurements.

References

[1]Landis, G. A., "Solar Cell Selection for Mars," *2nd World Conference on Photovoltaic Energy Conversion*, Vol. III, edited by J. Schmid, O. Ossenbrink, P. Helm, H. Ehmann, E. Dunlop, European Commission Joint Research Center, Luxembourg, 1998, pp. 3695–3698.

[2]Smith, P. H., Tomasko, M. G., Britt, D., Crowe, D. G., Reid, R., Keller, H. U., Thomas, N., Gliem, F., Rueffer, P., Sullivan, R., Greeley, R., Knudsen, J. M., Madsen, M. B., Gunnlaugsson, H. P., Hviid, S. F., Goetz, W., Soderblom, L. A., Gaddis, L., and Kirk, R., "The Imager for Mars Pathfinder Experiment," *Journal of Geophysical Research*, Vol. 102, No. E2, 1997, pp. 4003–4025.

[3]Smith, P. H., and Lemmon, M., "Opacity of the Martian Atmosphere Measured by the Imager for Mars Pathfinder," *Journal of Geophysical Research*, Vol. 104, No. E4, 1999, pp. 8975–8985.

[4]Thomas, N., Markiewicz, W. J., Sablotny, R. M., Wuttke, M. W., Keller, H. U., Johnson, J. R., Reid, R. J., and Smith, P. H., "The Color of the Martian Sky and Its Influence on the Illumination of the Martian Surface," *Journal of Geophysical Research*, Vol. 104, No. E4, 1999, pp. 8795–8808.

[5]Appelbaum, J., Landis, G. A., and Sherman, I., "Solar Radiation on Mars—Update 1991," *Solar Energy*, Vol. 50, No. 1, 1993, pp. 35–51.

[6]Rao, C. R., *Linear Statistical Inference and Its Applications*, 2nd ed., Wiley, New York, 1973, Chap. 2.

[7]Haykin, S., *Adaptive Filter Theory*, 2nd ed., Prentice-Hall, Upper Saddle River, NJ, 1991, Chap. 10.

[8]Markiewicz, W. J., Sablotny, R. M., Keller, H. U., and Thomas, N., "Optical Properties of the Martian Aerosols as Derived from Imager for Mars Pathfinder Midday Sky Brightness Data," *Journal of Geophysical Research*, Vol. 104, No. E4, 1999, pp. 9009–9017.